Photodiagnosis and Photodynamic Therapy 25 (2019) 472–479

Contents lists available at ScienceDirect

Photodiagnosis and Photodynamic Therapy

journal homepage: www.elsevier.com/locate/pdpdt

Utilizing photosensitizing and radiosensitizing properties of TiO_2-based mitoxantrone imprinted nanopolymer in fibrosarcoma and melanoma cells

Maryam Bakhshizadeh[a,1], Seyed Ahmad Mohajeri[b], Habibollah Esmaily[c], Seyed Amir Aledavood[d], Fatemeh Varshoei Tabrizi[e], Mahmoud Seifi[f], Farzin Hadizadeh[f], Ameneh Sazgarnia[a,*]

[a] Medical Physics Research Center, Mashhad University of Medical Sciences, Mashhad, Iran
[b] Pharmaceutical Research Center, Mashhad University of Medical Sciences, Mashhad, Iran
[c] Department of Biostatistics, School of Health, Mashhad University of Medical Sciences, Mashhad, Iran
[d] Cancer Research Center, Mashhad University of Medical Sciences, Mashhad, Iran
[e] Reza Radiotherapy and Oncology Center, Iran
[f] Biotechnology Research Center, School of Pharmacy, Mashhad University of Medical Sciences, Mashhad, Iran

ARTICLE INFO

Keywords:
Nanoparticles
Molecular imprinting
Titanium dioxide
Radiotherapy therapy
Photodynamic therapy

ABSTRACT

Background: Some materials such as TiO_2 display a luminescence property when exposed to X-ray radiation. Therefore, a proper photosensitizer can induce photodynamic effects by absorbing the emitted photons from these materials during radiotherapy. In this way, the problem of limited photo- penetration depth in photodynamic therapy is resolved. In this paper, following the production of a nanopolymer containing TiO2 cores and imprinted for mitoxantron (MIP), the possibility of utilizing its optical and radio properties on two lines of cancer cells were studied.

Methods: Mitoxantron (MX) was selected as the photosensitizer. The emission spectrum of the nanopolymers synthesized with/without MX was recorded during excitation by 6 MV X-rays. Also, the fluorescence signal of hydroxyl radicals produced into terephthalic acid medium by the nanopolymers were recorded during X irradiation. The percentage of cell survival following irradiation by X-rays was determined for various concentrations of drug agents by MTT assay. The synergistic index and IC_{50} were calculated to compare the findings.

Results: The emission spectrum of the nanopolymer reloaded with MX during X-ray irradiation indicated a considerable decline in comparison with the nanopolymer without MX. The level of free radicals produced by nanopolymer was significantly increased during irradiation with X-rays. The highest mean of synergistic indexes was observed in MIP.

Conclusion: The higher level of hydroxyl free radicals in MIP and lower cell viability in the DFW cell line as well as enhanced treatment efficiency confirm the hypothesis regarding the production of photodynamic effects by synthesized nanopolymer during radiotherapy.

1. Introduction

The treatment of malignant tumors has long been considered as one of the goals of the medical community, and various therapeutic approaches have been used for this purpose. Radiotherapy and chemotherapy are two such methods. Various types of malignancies respond differently to radiotherapy, so that some of them, including soft tissue fibrosarcoma and melanoma, may even be resistant to radiotherapy [1,2]. Chemotherapy drugs can help kill cancer cells, but they also exert deleterious effects on the whole body due to the non-specificity of the drugs and susceptibility to drug resistance, which limits their clinical application. To overcome these problems and improve the therapeutic effect of chemotherapy, attempts have been made to combine chemotherapy with radiotherapy and Photodynamic therapy (PDT). Combined therapy may induce a synergistic anti-tumor effect and reduce the therapeutic dose of chemotherapeutic drugs [3].

* Corresponding author at: Research Center of Medical Physics, Mashhad University of Medical Sciences, Mashhad, Iran.
E-mail addresses: bakhshizadehm1@thums.ac.ir (M. Bakhshizadeh), mohajeria@mums.ac.ir (S.A. Mohajeri), esmailyh@mums.ac.ir (H. Esmaily), aledavooda@mums.ac.ir (S.A. Aledavood), fatemehvarshoee@rroc.ir (F. Varshoei Tabrizi), SeifiM1@mums.ac.ir (M. Seifi), hadizadehf@mums.ac.ir (F. Hadizadeh), Sazgarniaa@mums.ac.ir (A. Sazgarnia).
[1] Present address: Torbat Heydariyeh University of Medical Sciences, Torbat Heydariyeh, Iran.

https://doi.org/10.1016/j.pdpdt.2019.02.006
Received 14 June 2018; Received in revised form 25 December 2018; Accepted 4 February 2019
Available online 06 February 2019
1572-1000/

PDT with minimal invasion is used for the treatment of accessible lesions (either superficial or deep) with repeatability. In this method, after injecting an appropriate drug (photosensitizer) into the body, the tumor area is exposed to radiation of proper wavelengths. Excitation of a photosensitizer leads to its lowest energy triplet state, which has a sufficiently long lifetime to allow for bimolecular reactions with substrate molecules. Electron or hydrogen transfer reactions from the triplet state of the photosensitizer eventually lead to superoxide anion and hydroxyl radicals (type I reaction), or energy transfer to molecular oxygen will generate singlet O2 (type II reaction). So that photosensitization in the presence of cellular oxygen and the production of free radicals lead to the cell death. Therefore, photodynamic therapy requires the simultaneous presence of three factors: light, photosensitizer and oxygen [4]. Nonetheless, the main limitation of PDT is the limited depth of light penetration in the tissue, which is at best 1 Cm [4]. One effective way to address this limitation is to combine radiotherapy and photodynamic therapy. In this way, nano-scintillator and photosensitizer are merged. When nanoparticles are exposed to ionizing radiation (e.g. X-rays), luminescence process is occurred by nanoparticles, which activates photosensitizing molecules into producing free radicals. This increases the radiotherapy efficiency induced by the photodynamic therapy. In other words, the nanoparticle plays the role of a transducer. In this case, nanoparticles in addition to their ability to increase radiotherapy efficiency due to their radiosensitizing effect, act as the internal light sources, and thus the limitation of low penetration depth of light in photodynamic treatments is resolved. Moreover, a combination of radiotherapy and photodynamic therapy augments the therapeutic efficacy. It should be noted that the emission spectrum of stimulated nanoparticles must be compatible with the absorption spectrum of photosensitizer [5].

Many studies have explored the quality of this process and optimized the occurrence conditions of this combined therapy. For example, scintillation nanoparticles LaF3: Tb3 + stimulated by X-ray emit a green light, which can stimulate meso-tetra (4-carboxyphenyl) porphyrin (MTCP), and is often used in photodynamic therapy [6]. The singlet oxygen production of MTCP was low in the presence of X-rays, but the singlet oxygen production was dramatically increased under X-ray when MTCP was conjugated with LaF3: Tb3 + nanoparticles [6,7]. LaF3: Ce3 + / DMSO / PPIX / PLGA microshells may incur sublethal damages, but they can produce oxidative stress when exposed to X-rays [8]. The Cu-Cy nanocomplex as a photosensitizer stimulated by X-ray absorbing has been used in vivo and in vitro studies [9].

TiO2 nanoparticles can also be considered as a scintillator and their application in this combined therapy needs to be further studied, though few studies have explored this area so far.

In the first part of this study, a molecular imprinting technique was used to combine the TiO2 nanoparticles and photosensitizers. In molecular imprinting process, the monomers should interact with template and form a complex through non-covalent bonds. Thus, the template molecule should have proper functional groups to interact with the functional monomers. Also, the template molecule needs to be stable at high temperatures (about 60 °C) when polymerization is carried out. Among photosensitizers that their absorption spectrum approximately matches the emission spectrum of TiO2 nanoparticles, the mitoxantrone (MX) chemotherapy drug has essential imprinting condition. MX is a synthetic anthracenedione. Anthracyclines undergo efficient enzymatic one electron reduction to semiquinone radicals and take part in the cellular redox cycling reactions. Generation of superoxide radicals and the formation of highly toxic hydroxyl radicals have been demonstrated to occur during redox cycling of anthracyclines. MX has two major absorption peaks at 610 and 660 nm, it can be an effective photosensitizer for PDT [1]., so that the mitoxantrone can absorb the light released from the nanoparticles and induce a photodynamic event. On the other hand, in the structure of this polymer nanocomplex, biodegradable connecting monomers have been used, which keeps these two together as a drug delivery system.

Different polymers were produced and the optimum polymer was selected based on the drug loading and drug delivery rate. In composite synthesis, the monomer polymer was selected in a way that loaded drug delivery was greater in low pHs (a characteristic of cancer cells) compared to high pHs (a prop characteristicerty erty of healthy cells) [10]. FT-IR was used to ensure mitoxantrone imprintined in the polymer and the EDS method was applied to confirm the TiO2 trapping inside the nanostructure.

The nanocomposites were exposed to X-rays radiation and the level of hydroxyl radicals generated under all conditions was measured in the aqueous medium using a terephthalic acid dosimeter. It was followed by an in vitro study of melanoma cell lines and human fibrosarcoma. In addition to examining the cytotoxicity of all therapeutic agents, the efficacy of combined therapies was also determined.

2. Materials and methods

2.1. Cell lines

DFW cell line is a humanized pigmented subtype derived from the DFB cell line, which is considered as melanoma cell lines. The HT 1080 cell line was also derived from fibrosarcoma tumor of a 35-year-old Caucasian male. Cell lines were provided by Pasteur Institute of Iran.

2.2. Chemicals

Titanium dioxide nanoparticles of 30 to 50 nm were purchased from US Research Nanomaterials Inc. and Mitoxantrone was obtained from Santa Cruz, USA. Methacrylic acid (MAA) and terephthalic acid were also purchased from Sigma-Aldrich Company, Germany. Acryloyl chloride and triethylamine were acquired from the Merck, Germany and the Azobisisobutyronitrile (AIBN) was purchased from Acros Company, Belgium. All solvents including acetonitrile (ACN), methanol, chloroform, acetone, acetic acid and dichloromethane were of HPLC Grade. The double-distilled deionized water was used.

2.3. Methods

2.3.1. Design and synthesis of polymer nanocomplex

According to the emission spectrum of TiO2 nanoparticles stimulated by X-ray, the mitoxantrone was selected as a photosensitizer. The following steps were taken to prepare a composite with Titanium Dioxide Nanoparticles as its core and mitoxantrone imprinted polymer (MIP) in its surrounding.

TiO2 nanoparticles were activated by MAA. The biodegradable connective monomer of diacrylated polycaprolactone was obtained from the reaction of polycaprolactone diol with acrylic chloride. Methacrylic acid (MAA) as a monomer agent (300 µmol) and mitoxantrone (7.5 µmol) as a mold molecule were dissolved in a closed and sealed tube containing 0.5 ml of DMSO and 5 ml of chloroform solution. The solution was stored at 4 °C for 1 h. Then, 0.36 g of activated nanoparticles of titanium dioxide (TiO2-MAA) were dispersed in 0.5 ml of DMSO, sonicated for 10 min, and added to the mixture. In the next step, they were stirred at a speed of 100 rpm at room temperature for 1 h. At this stage, diacrylated polycaprolactone (1.58 g) as a connective monomer and AIBN as the initiator of the polymerization reaction were added to the solution. Each tube was then sonicated and sparged with oxygen-free nitrogen for 5 min. The tube was then completely sealed and placed at 60 °C for 22 h to complete the radical polymerization reaction. Finally, samples were washed with a mixture of water and acetic acid (9:1, v/v) and water-DMSO (9:1, v/v) and then centrifuged (at a speed of 300 rpm for 10 min) until the polymer molecules were separated and it was impossible to measure them by the UV/VIS spectrophotometer.

Non-imprinted polymers (NIPs) were synthesized without mold molecules under conditions identical to that of MIP.

To record emission spectrum, washed (lacking MX) and non-washed (containing MX) MIP and NIP polymers with a concentration of 2 mg/ml were dispersed in deionized distilled water. 1cc of each sample was exposed to X-ray (field size: 10 × 10, on the flat surface, SSD = 100, dose rate: 200 cGy/min and dose of 100 cGy) in the quartz cuvette. During radiation, the emission spectrum of samples was measured and recorded by the Spectrometer (AvaSpec-2048 Dual Thermo-Electric Cooled Fiber Optic) made in the Netherlands (8 nm resolution, 4 scans of 250 ms per second).

2.4. Chemical dosimetry of hydroxyl radicals

0.33 mg/ml of terephthalic acid and 0.2 mg/ml of NaOH in water were used as a chemical dosimeter to quantify the hydroxyl radicals produced in aqueous conditions. If the terephthalic acid reacts with radicals in the medium excited with a light of 310 nm, it will emit fluorescence spectrum at 420 nm. Thus, the intensity of emission is proportional to the amount of hydroxyl radicals generated in the aqueous medium [11].

To determine the level of radicals produced by drug agents, each drug agent was dispersed separately in a chemical dosimeter solution. For each agent, three separate specimens were prepared for reiteration. The specimens were stimulated by spectrofluorimeter at a wavelength of 310 nm and the emission spectrums were recorded in a range of 350–500 nm (stimulation monochromator bandwidth of 20 nm and emission monochromator bandwidth of 10 nm).

To determine the amount of free radicals produced by X-rays in the presence of various drug agents, specimens identical to the above samples were prepared and subject to X-rays (field size 10 × 10, on the flat surface SSD = 100, dose rate: 200cGy /min, dose: 100 cGy). The light emission was recorded by a spectrofluorometer under corresponding conditions.

Then, in all groups, a comparison was drawn between the amount of hydroxyl radicals produced in the aqueous medium with and without X-ray irradiation.

2.5. In vitro studies

After preparing DFW and HT1080 cell lines, the cells were first defrozen and then transferred to cell culture flasks and placed in a 37 °C incubator containing CO_2. Every 2–3 days, their culture medium was swapped with a new medium. When the cells covered the surface of the flask as a single layer, 0.25% EDTA Trypsin solution was used to separate cells from the flask.

Then, cells were counted by trypan blue method, and then divided and subject to different experiments. The percentage of cell survival was evaluated by MTT assay. For this purpose, the contents of wells were drained and 100 µl culture medium without FBS and then 10 µl MTT solution was added. Plates were incubated for 4 h after which the environment containing MTT was drained and 200 µl of DMSO solvent was added to each well. Finally, the amount of pigment generated was measured by ELISA reader (Stat Fax-2100 Awareness, Mountain View, CA, USA) at a spectrum of 540 nm and 630 nm.

2.6. Determining the cytotoxicity of agents

In each cell line, 24 h after counting and dividing cells in 96-well plates, various drug agents, each with at least four different concentrations, were incubated for 90 min [12] and then washed by PBS.

2.7. Evaluation of X-ray cytotoxicity

Also, to determine the toxicity of x-rays, cells that contained four concentrations of each drug agent or lacked any drug agent were subject to X-ray radiation with 6 different doses (50, 100, 200, 400, 600, and 800 cGy). For the purpose of radiation, SSD was first placed on a 100 Cm treatment bed and then 1.5 cm of bolus (equivalent to energy build-up depth of 6 MV) was inserted on the bed. A field of 10 × 10 and Gantry angle of 180° was set. To determine the percentage of cell survival, MTT assay was performed after one week. The incubation with drug and polymers lasted for 90 min. After washing with PBS, plates were exposed to X-rays with a dose of 100 cGy. The cell survival was then computed after a week.

2.8. Data analysis

The intensity of the light emission of MIP and NIP samples loaded with/without MX were recorded during X-ray irradiation. After integrating the spectra for each sample, their graph was also plotted.

The signals emitted from the dosimeters containing TA with/without agents were recorded and emission spectrum was plotted for the purpose of comparison.

The mean cell survival percentages in each experimental group were calculated in different treatment groups.

IC_{10} and IC_{50} values and the synergistic index were defined and calculated as follows.

IC_{10}: Concentration or dosage of a therapeutic agent causing the death of 10% of cells was defined as IC_{10}.

IC_{50}: Concentration or dosage leading to the death of 50% of cells was defined as IC_{50}.

Synergistic Index: It is defined as the ratio of real cell death to expected cell death. It was calculated as below:

The cell deaths caused by X-rays in the presence of a therapeutic agent were divided by the sum of toxicity-induced cell deaths and X-ray radiation separately.

Statistical analysis was performed by SPSS 16. The results of Kolmogorov-Smirnov test confirmed the normal distribution of data. A significance level of 0.05 was assumed for comparison. All graphs were plotted by Excel software.

One-way ANOVA and Dunnett's T3 test were used to compare the groups.

3. Results

In this section, first the data obtained from characterization of nanostructures and the emission spectrum of various agents during stimulation by X-ray are presented and then the hydroxyl radicals produced in the TA dosimeters are shown, followed by the findings of cellular experiments.

3.1. Characterization of the nanostructures

The size of molecularly imprinted polymer (MIP) particles was evaluated using SEM, TEM and XRD. The XRD spectrum of MIP composite is shown in Fig. 1.

Differential peaks at 27, 36 and 55° angles indicate the presence of TiO_2 and peaks at 21, 22, 23, 27, 36, 41, and 54° exhibit the polymer structure.

According to the results of XRD, the size of TiO2 nanoparticles was in the range of 43 to 53 nm, which was increased to 59–69 nm after applying the molecular imprinting technique and creating polymer coating (size of nanoparticles obtained from debye Scherrer equation). According to SEM image (Fig. 2a), the size of TiO_2 nanoparticles (TiO_2 NPs) was less than 50 nm and the synthesized MIP size was about 50–75 nm (Fig. 2b). The TEM image taken from MIP also confirmed these results. The average size of nanoparticles reported by TEM was 62.8 ± 7.7 nm (Fig. 3).

3.2. Recording emitted Fluorescence and chemical dosimetry during X-Ray exposure

The emission spectra of the washed MIP (MX-free), and unwashed

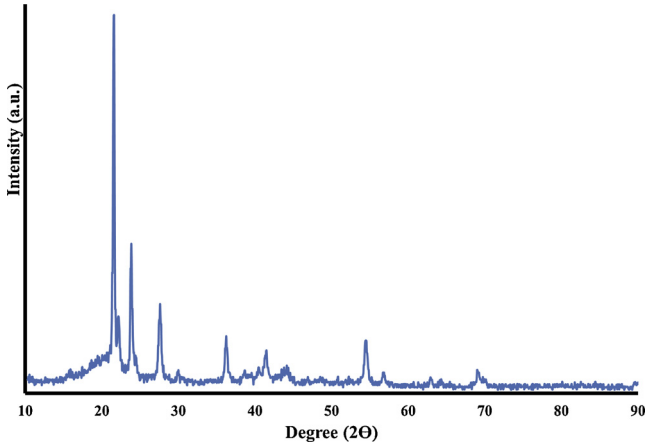

Fig. 1. XRD spectrum of MIP composite.

MIP (containing MX) during X-ray emission are presented in Fig. 4. It is observed that when MX is present in the structure of MIP, the intensity of emission drops. The NIP emission spectrum before and after MX loading was recorded during X-ray irradiation, as shown in Fig. 5.

Fig. 6 shows the emission spectrum of the drug agents in a medium containing a chemical dosimeter (TA). As stated above, the intensity of emission is proportional to the amount of free radicals produced in the aquatic environment.

The highest amount of hydroxyl radicals was produced by MIP and NIP, respectively. MX polymer and TiO2 polymer failed to produce measurable amounts of radicals.

Fig. 7 shows the emission spectrum of drug agents in a medium with chemical dosimeter (TA) after X-ray exposure, which indicates the amount of free radicals generated during x-rays exposure. It shows the repetition of the same trend, but the intensity emission peak at MIP and NIP was increased by about 100 units after stimulation by X-rays. It should be noted that the X-ray dose used in this study generated a small amount of measurable radical hydroxyl.

3.3. Determining cytotoxicity of chemical agents and X-ray

In Fig. 8, the curve of average cell survival at different doses of radiation is presented for two cell lines.

In the DFW cell line, with a dose increase of up to 400 cm, the percentage of cell survival drops, after which no significant decline occurs. However, in the HT1080 cell line, a steady and significant decrease in cell survival is observed with the elevated dose of radiation. Except for a dose of 50 with 100 cGy ($P = .769$), all groups demonstrated a significant differences compared to the control group ($P < 0.001$).

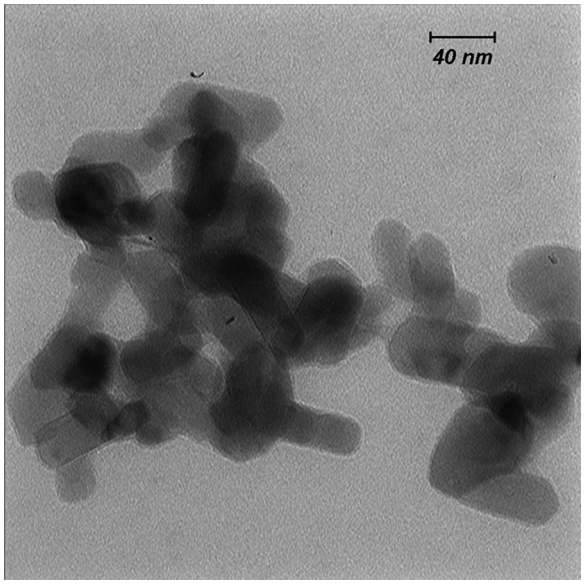

Fig. 3. TEM image of MIP composite.

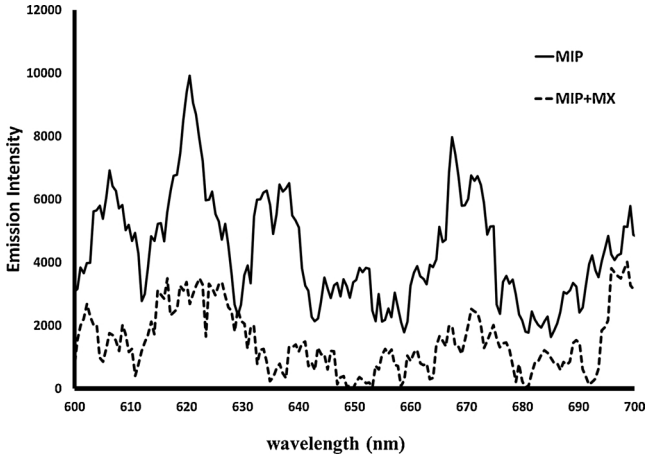

Fig. 4. The emission spectra of washed and unwashed MIP (without and with MX during irradiating by X-ray.

Based on these results, in DFW cell line, $LD_{10} = 70$ and $LD_{50} = 290$ cGy, and in HT1080 cell line, $LD_{10} = 20$ and $LD_{50} = 400$ cGy were achieved.

The effect of concentration variations of TiO_2 polymer in the presence and absence of X-rays on the mean survival rate is shown in

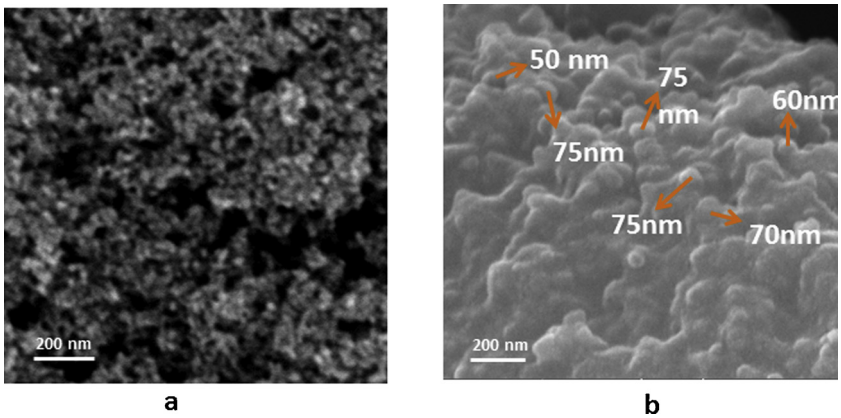

Fig. 2. SEM images of TiO_2 nanoparticles on the left and MIP composite on the right.

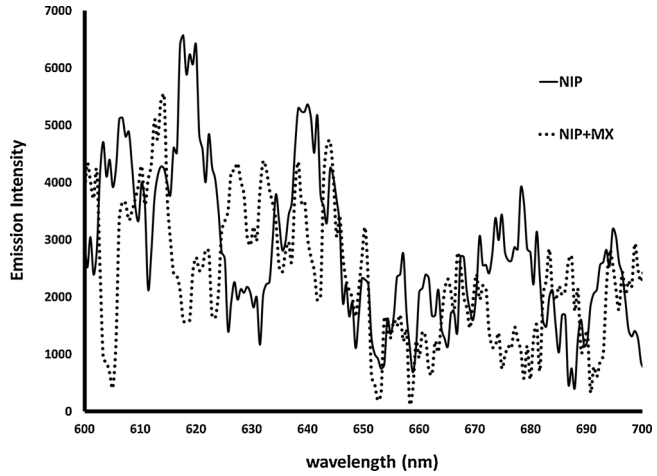

Fig. 5. The emission spectra of NIP without and with MX during irradiating by X-ray.

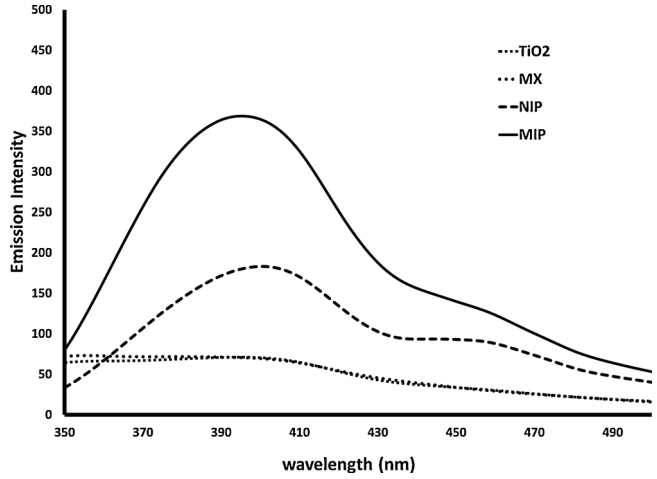

Fig. 6. The emission spectrum of chemical dosimetry (TA) in the presence of the agents (excitation wavelength of 310 nm, with a bandwidth of 20 nm, and emission monochromator bandwidth of 10 nm; the data is based on the mean of 3 repetitions of experiments).

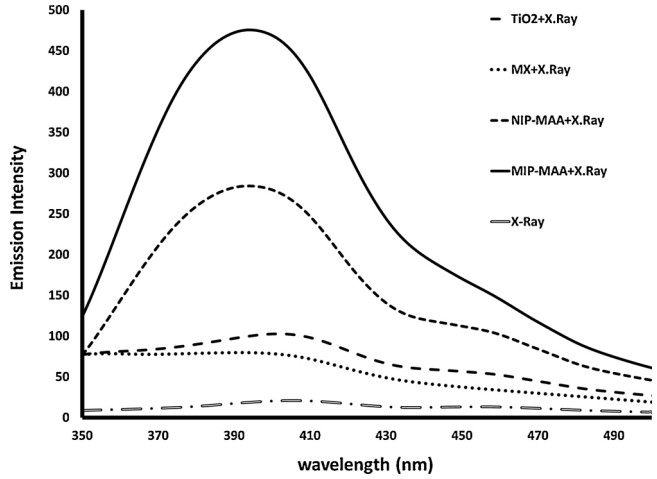

Fig. 7. Emission spectra of chemical dosimetry (TA) in the presence of drug agents after exposure by 100 cGy X-ray (excitation wavelength was 310 nm with a bandwidth of 20 nm and emission monochromator bandwidth of 10 nm). The data were obtained after three reiterations of the experiments.

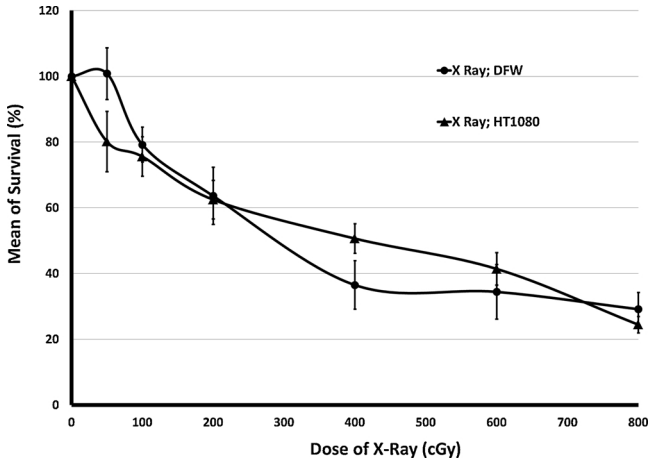

Fig. 8. Average curve of cell survival ± standard deviation in different doses of x-ray (dose rate: 200 cGy/min, dose: 100 cGy) on DFW and HT1080 cell lines. The data were obtained from at least 4 reiterations of the experiments.

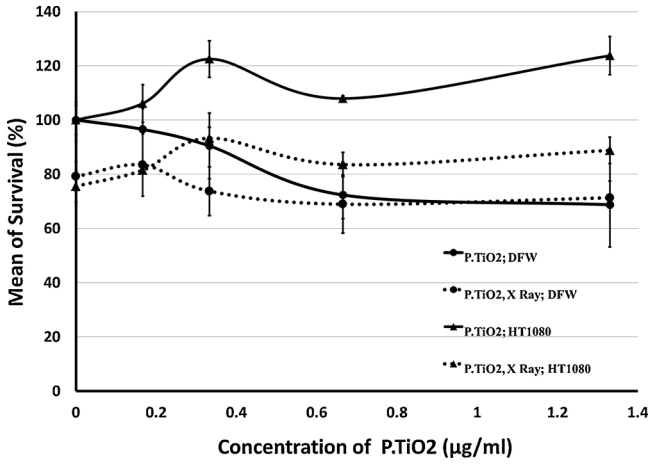

Fig. 9. Average cell survival ± standard deviation in different concentrations of $P.TiO_2$ in the presence and absence of X-rays (doe rate: 200 cGy/min; dose: 100 cGy) on the DFW and HT1080 cell lines. The data were obtained after at least 4 repetitions of experiments.

Fig. 9.

As can be seen, with increased $P.TiO_2$ concentration in the DFW cell line, the percentage of cell survival dropped. Concentrations of 0.67 and 1.33 µg/ml relative to the control group and relative to a concentration of 0.17 µg/ml induced a significant decline in cell survival percentage ($P < 0.05$). Also, a concentration of 1.33 µg/ml compared to 0.33% µg/ml also significantly reduced the survival ($P = 0.02$). However, after X-ray application, no significant difference was observed between different concentrations ($P < 0.05$).

As for HT1080 cell line, all concentrations of this polymer increased cell survival, and it was significant at 0.67 and 1.33 µg/ml ($p < 0.05$) concentrations while other concentrations were not significantly different ($P > 0.05$). In the presence of X-rays, 0.17 and 1.33 µg/ml concentrations induced significant survival decline compared to the control group.

The effect of concentration variations of MX in the presence and absence of X-rays on the mean survival rate is depicted in Fig. 10.

In the DFW cell line, a marked decrease in survival percentage is observed by elevated concentration of MX. The control group has shown the significant differences compared to the all groups ($P < 0.01$). Also, there were significant differences between the different groups in the all concentrations, except for the groups receiving the MX at the concentrations of 0.005 with 0.01 and 0.02 with 0.03 and

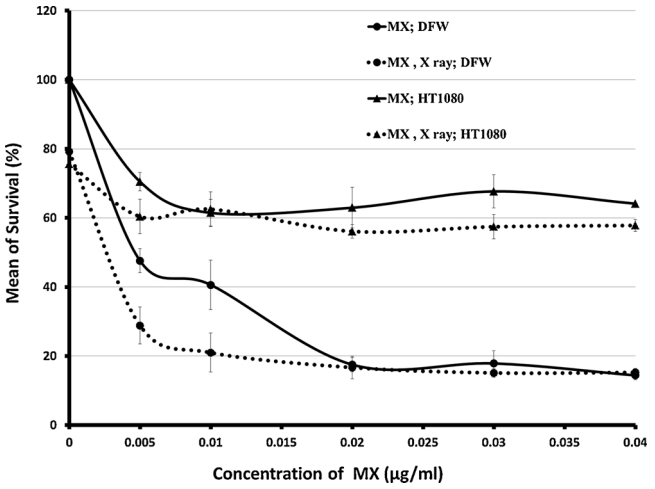

Fig. 10. Average cell survival ± standard deviation in different concentrations of MX in the presence and absence of X-rays (dose rate: 200 cGy /min, dose: 100 cGy) on DFW and HT1080 cell lines. The data were obtained after at least 4 repetitions of the experiments.

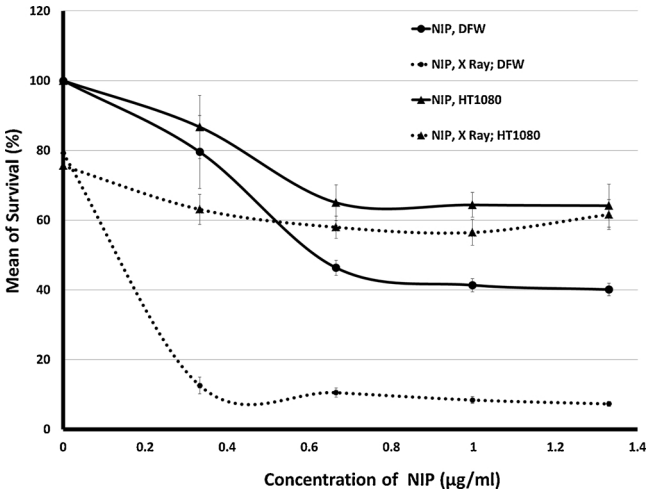

Fig. 12. Average cell survival percentage ± standard deviation in different concentrations of NIP in the presence and absence of x-rays (dose rate: 200 cGy /min; dose: 100 cGy) on DFW and HT1080 cell lines. The data are based on at least 4 replicates of the experiments.

0.04 (µg/ml). The toxicity of MX on the HT1080 cell line was increased to a concentration of 0.01 (µg/ml), after which increasing concentration did not decrease the cell survival significantly ($P < 0.05$), but reduced survival percentage was significant compared to the control group ($P < 0.001$).

In the presence of X-rays, for all concentrations expect 0.0007 (µg/ml) in the DFW cell line, there was a significant reduction in survival percentage compared to the control group ($P < 0.001$). Decreased cell survival at all concentrations was also significant compared to a concentration of 0.0007 µg/ml ($P < 0.001$). Concentrations of 0.02, 0.03 and 0.04 also caused a significant drop ($p < 0.026$) relative to the concentration of 0.005 µg/ml ($P < 0.026$). Concentration of 0.02 relative to 0.01 (µg/ml) induced a significant reduction ($P = 0.05$). However, in the HT1080 cell line in the presence of X-rays, there was a significant reduction in all concentrations compared to the control ($P < 0.05$). Also, concentrations of 0.02, 0.03 and 0.04 (µg/ml) prompted a significant drop compared to 0.0015 (µg/ml) ($P < 0.05$). Decreased survival was significant at concentrations of 0.03 and 0.04 (µg/ml) compared to 0.01 µg/ml ($P < 0.05$).

As shown in Fig. 11, in case of MX polymer in the DFW cell line, the increased concentration leads to diminished survival. Concentration of 0.29 (µg/ml) compared to the control group and concentrations of 0.07 and 0.14 (µg/ml) led to a significant reduction in survival ($P < 0.05$). Concentration of 0.58 (µg/ml) also caused a significant reduction in comparison to the control group and concentrations of 0.07 and 0.14 (µg/ml) ($P < 0.05$). In the HT1080 cell line (Fig. 11), by increasing the concentration of MX to 0.29 (µg/ml) the cell survival fell initially, but it then picked up. This rise and fall was significant at all concentrations except 0.07 (µg/ml) ($P < 0.001$).

In the DFW cell line, the polymer at all concentrations increased the killing effect of radiation compared to the control group, significantly ($P < 0.001$). There were no significant difference between the other groups receiving the polymer ($P > 0.05$), except for the concentration of 0.58 (µg/ml) in comparison with the 0.07 and 0.15 (µg/ml). In the presence of X-ray, the survival percentage of the HT1080 cell line at concentrations greater than 0.29 (µg/ml) was significantly higher than the control group ($P < 0.05$). However, X-ray radiation did not significantly change in the presence of MX polymer (Fig. 11).

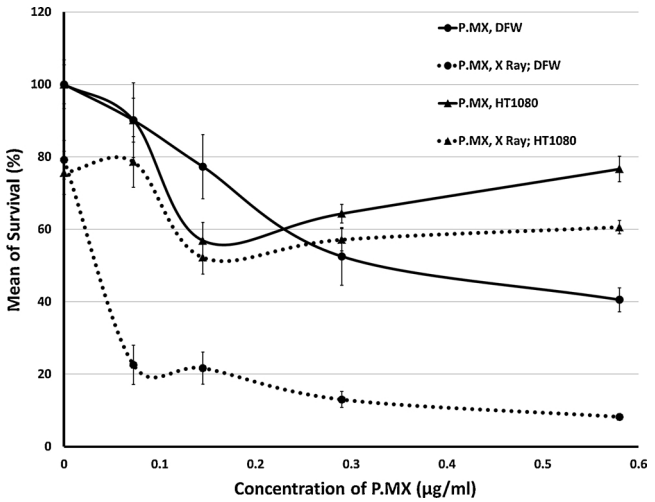

Fig. 11. Average cell survival percentage ± standard deviation in different concentrations of P.MX in the presence and absence of X-rays (dose rate: 200 cGy /min; dose: 100 cGy) on DFW and HT1080 cell lines. The data were obtained after at least 4 repetitions of the experiments.

Fig. 12 shows the non-imprinted polymer (NIP) toxicity with/without X-ray radiation. The increased NIP concentration prompts a significant drop in the survival of the DFW cell line ($P < 0.05$), but in the case of the HT1080 cell line, this trend is slower, so that with elevated concentration (up to 0.67 µg/ml), the survival falls for a while, after which it remains almost constant. In this cell line, concentrations of 1.67, 1 and 1.33 (µg/ml) were significantly lower than the control group and concentration of 0.17 µg/ml had a significant effect on cell survival ($P < 0.01$). Although all concentrations were not the same, but this difference was not significant ($P < 0.05$).

In the presence of X-rays, all concentrations caused a significant reduction in the survival of the DFW cell line ($P = 0.000$), and cell survival reduction at a concentration of 1.33 µg/ml was significant compared to concentrations of 0.33 and 0. 67 (µg/ml) ($P < 0.027$). Also in the HT1080 cell line, after exposure to X-rays, concentrations of 0.33, 0. 67, 1, and 1.33 (µg/ml) induced a fall in the cell survival compared to control and concentration of 0.17 (µg/ml) ($P < 0.01$).

In Fig. 13, the average cell survival is observed at various concentrations of MIP with/without X-ray radiation.

MIP toxicity on the DFW cell line was insignificant initially ($P = 0.304$), but it then picked up significantly ($P < 0.001$) compared to the control group. In the HT1080 cell line, however, with increased concentration of the imprinted composite, a significant drop was observed in the control group ($P < 0.01$).

In both cell lines and at all concentrations, the presence of MIP

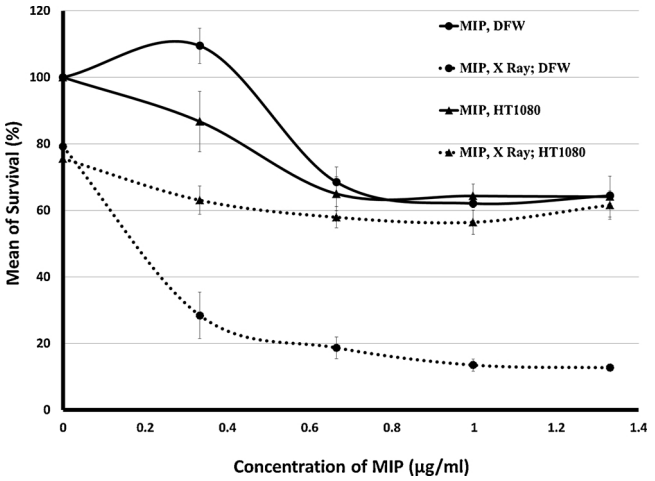

Fig. 13. Average cell survival ± standard deviation in different concentrations of MIP in the presence and absence of X-rays (dose rate: 200 cGy / min, dose: 100 cGy) on DFW and HT1080 cell lines. The data are based on at least 4 repetitions of the experiments.

heightened the effect of X-rays. All concentrations promoted a significant fall compared to control ($P < 0.001$), but this decrease was higher in the DFW cell line.

3.4. Synergistic Index, IC10 and IC50

The mean X-ray synergistic index with various drug factors is presented in Table 1. The highest value was observed in the presence of MIP in the DFW cell line.

Based on the results of this study, in the DFW cell line, the concentrations of TiO_2 polymer and MIP polymers are lower than IC_{50}, and if any of these factors is intended to reduce the survival by 50%, it is necessary to employ a concentration higher than the maximum concentrations used in this study. In the HT1080 cell line, the concentrations utilized in this study were unable to induce a 50% reduction in cell survival in all groups. In the case of TiO_2 polymer, even a 10% reduction in cell survival was not obtained.

4. Discussion

In light of the reduced emission intensity recorded on samples containing MIP and NIP after MX loading with X-rays, it can be concluded that photons emitted from TiO_2 nanoparticles excited by X-ray, which are in the nucleus of nanocomposites, are well absorbed by MX molecules. Hence, this nanocomposite can be used to connect and transport these two materials. According to the results, it is expected that TiO_2 nanoparticles act as light sources for excitation of MX sensitizer provided that this nanocomposite is stimulated by X-rays in oxygen-enriched environments [13].

Table 1
The synergistic index, IC_{10} and IC_{50}.

Agent	Synergistic Index ± standard deviation		IC10 (µg/ml)		IC50 (µg/ml)	
	Cell line					
	DFW	HT1080	DFW	HT1080	DFW	HT1080
TiO_2 polymer	0.7 ± 0.1	1.9 ± 1.2	0.139	> 1.33	> 1.33	> 1.33
MX	0.9 ± 0.1	0.7 ± .01	0.0007	0.0015	0.0040	> 0.04
MX polymer	1.7 ± 0.6	0.7 ± 0.1	0.0725	0.0700	0.3100	> 0.58
NIP	1.4 ± 0.5	0.7 ± 0.2	0.1700	0.2800	0.6100	> 1.33
MIP	2.7 ± 2.4	1.0 ± 0.1	0.5000	0.2800	> 1.33	> 1.33

The mean X-ray synergistic index with the agents at different concentrations ± standard deviation and IC10 and IC50 for DFW and HT1080 cell lines.

Studies on the level of hydroxyl radicals produced in the aqueous medium shows that the MIP and NIP nanocomposites can produce free radicals in the aqueous medium, and this amount can be increased by stimulation with X-rays.

In concentrations of TiO2 nanoparticles and MX, even in the presence of X-rays, they have failed to produce a significant amount of free radicals detectable by TA, but they were synthesized in nanocomposites that connected them. A large sum of free radicals is produced, which is higher than the sum of radicals generated by each of these two agents. This is despite the fact that free radicals produced by TiO2 or MX polymers are negligible and cannot be measured by this technique. On the other hand, although X-rays do not produce or record a radically measurable amount of hydroxyl, the amount of radicals generated in nanocomposites was increased dramatically after X-ray stimulation. Therefore, this extra effect may be attributed to the free radicals produced from photodynamic therapy during radiotherapy.

Given the toxicity of various drug factors on the DFW cell line and IC_{10} and IC_{50}, it can be predicted that concentrations of TiO_2 polymer and MIP are lower than their IC_{50}, and if any of these factors is intended to reduce survival by 50%, a concentration above the maximum concentrations utilized in this study is required.

The polymer coating of MX was able to reduce MX toxicity. Considering that polymers are biodegradable [14], this polymer structure could be used as a delivery system for MX drugs in chemotherapy. TiO2 nanoparticles are not purely administrable, therefore this polymer could be a good alternative for administration of these nanoparticles in necessary cases.

In light of the above findings about the effect of radiation in the presence of pharmaceutical agents, it can be stated that the polymer structure of TiO2 nanoparticles is not sensitive to radiation. This is not consistent with the results of studies about radiation sensitivity in titanium dioxide nanoparticle (e.g. Rezaei et al. 2013), which indicate the radiation sensitivity of TiO_2 nanoparticles at concentrations greater than 10 (µg/ml) on MCF-7 and MKN-45 cell lines in a dose of 200cGy X-ray. This difference could be due to polymerization, modified concentrations, cell line differences, or dose of radiation in two studies.

We did not observe any significant sensitivity in MX concentrations, but when it is prescribed in the form of a polymer, its radiosensitivity could be detected. Sazgarnia et.al also reported the effects of radiosensitivity of mitoxantrone hydrochloride exposure on the MCF-7 cell line in 2012 [15]. Therefore, to observe the effects of MX radiosensivity, its pure form should not be used. This could be attributed to the high toxicity of its pure form, which prevents the observation of additional effects in combination therapies.

NIP and MIP structures in the presence of X-rays are synergistic. This effect could be due to their sensitivity to radiation and photodynamic therapy during radiation, as these polymer composites contain TiO2 (as a source of light after X-ray stimulation) and MX as an optical sensitizer.

In the HT1080 cell line, although the average synergistic index is larger than one, none of the drug agents was able to increase radiotherapy efficiency and cause radiation sensitivity. In other words, the increased synergistic index in these cases was due to elevated cell survival under the influence of the drug agent. It seems that in this cell line, the treatment has not been successful and this technique has failed to increase the radiotherapy efficiency in this cell line. This is not in agreement with the results of this study on the DFW cell line, which can be due to the greater resistance of this cell line to various treatments. As demonstrated, this category is even more resistant to MX chemotherapy than DFW.

Considering the toxicity of various drug factors and their IC_{10} and IC_{50} values in the HT1080 cell line, it can be contended that in all groups, IC_{50} value of this cell line is higher than concentrations used in

the study. The MX polymer in this cell line has also been able to reduce the toxicity of MX. Therefore, this polymer structure can be used as a delivery system for MX drugs in chemotherapy. Based on the results of this cell line, polymer can also be used to administer TiO2 nanoparticles.

The MX drug on the DFW cell line induces a better response than the HT1080 cell line. Therefore, chemotherapy with MX will be more effective in this cell line. The response rate of the two cell lines is identical to that of radiotherapy. However, in the combined therapy considered in this study, the HT1080 cell line is more resistant and the treatment method will be more effective in treating DFW. Given that melanoma tumors are relatively resistant to radiotherapy [1,16], it is anticipated that this combined therapy increases the therapeutic efficacy. With regard to the HT1080 cell line, due to its resistance to chemotherapy and radiotherapy, optimal therapeutic factors such as drug concentrations could be achieved.

More studies are need to find relation between the amount of radicals produced, and cytotoxicity because of behavior of cells could be different. Generating another reactive species also should be evaluated.

5. Conclusion

In the study of therapeutic properties of this nanocomposite in aqueous and cellular media during excitation with X-rays, the emission spectrum of the MIP sample (MX removal from the nanocomposite), which seems to be related to TiO2 nanoparticles in MIP core, was recorded After loading MX on the MIP and stimulating it with the X-Ray, the intensity of the previous emission peaks was reduced, and the light absorption of the TiO_2 nanoparticles contained in the core of the structure by the MX template molecule in the MIP structure was confirmed. Therefore, it seems that this structure offers an appropriate alternative for using photodynamic effects during radiotherapy. To test this assumption, the amount of free radicals produced before and after X-ray irradiation was measured by a TA dosimeter. It was observed that the sum of free radicals after radiation had dropped significantly compared to the non-radiation sample and X-rays alone. This increased radical production can be attributed to radicals generated by photodynamic events during radiotherapy. In light of the effect of MIP, the results of these therapies on DFW and HT1080 cell lines also confirmed the hypothesis of photodynamic therapy during radiotherapy by nanocomposites. This polymer structure is also able to reduce the toxicity of MX.

Acknowledgment

The data presented in this report is a part of a PhD thesis that was financially supported by the Research Deputy of Mashhad University of Medical Sciences, Mashhad, Iran.

References

[1] A. Sazgarnia, et al., Photosensitizing and radiosensitizing effects of mitoxantrone: combined chemo-, photo-, and radiotherapy of DFW human melanoma cells, Lasers Med. Sci. (2013) 1–7.
[2] B. Windeyer, S. Dische, C.M. Mansfield, The place of radiotherapy in the management of fibrosarcoma of the soft tissues, Clin. Radiol. 17 (1) (1966) 32–40.
[3] Q. Zhang, L. Li, Photodynamic combinational therapy in cancer treatment, JBUON 23 (3) (2018) 561–567.
[4] M.B. Ericson, A.-M. Wennberg, O. Larkö, Review of photodynamic therapy in actinic keratosis and basal cell carcinoma, Ther. Clin. Risk Manag. 4 (1) (2008) 1.
[5] D.K. Chatterjee, L.S. Fong, Y. Zhang, Nanoparticles in photodynamic therapy: an emerging paradigm, Adv. Drug Deliv. Rev. 60 (15) (2008) 1627–1637.
[6] P. Juzenas, et al., Quantum dots and nanoparticles for photodynamic and radiation therapies of cancer, Adv. Drug Deliv. Rev. 60 (15) (2008) 1600–1614.
[7] Y. Liu, et al., Investigation of water-soluble x-ray luminescence nanoparticles for photodynamic activation, Appl. Phys. Lett. 92 (4) (2008) p. 043901-043901-3.
[8] X. Zou, et al., X-ray-induced nanoparticle-based photodynamic therapy of cancer, Nanomedicine 9 (15) (2014) 2339–2351.
[9] L. Ma, X. Zou, W. Chen, A new X-ray activated nanoparticle photosensitizer for cancer treatment, J. Biomed. Nanotechnol. 10 (8) (2014) 1501–1508.
[10] V. Vukovic, I. Tannock, Influence of low pH on cytotoxicity of paclitaxel, mitoxantrone and topotecan, Br. J. Cancer 75 (8) (1997) 1167.
[11] A. Sazgarnia, A. Shanei, Evaluation of acoustic cavitation in terephthalic acid solutions containing gold nanoparticles by the spectrofluorometry method, Int. J. Photoenergy 2012 (2012).
[12] A.-R. Montazerabadi, et al., Mitoxantrone as a prospective photosensitizer for photodynamic therapy of breast cancer, Photodiagn. Photodyn. Ther. 9 (1) (2012) 46–51.
[13] N.Y. Morgan, et al., Nanoscintillator conjugates as photodynamic therapy-based radiosensitizers: calculation of required physical parameters, Radiat. Res. 171 (2) (2009) 236–244.
[14] K.-S. Lee, D.S. Kim, B.S. Kim, Biodegradable molecularly imprinted polymers based on poly (ε-caprolactone), Biotechnol. Bioprocess Eng. 12 (2) (2007) 152–156.
[15] A. Sazgarnia, et al., In vitro survival of MCF-7 breast cancer cells following combined treatment with ionizing radiation and mitoxantrone-mediated photodynamic therapy, Photodiagn. Photodyn. Ther. (2012).
[16] P. Strojan, Role of radiotherapy in melanoma management, Radiol. Oncol. 44 (1) (2010) 1–12.